Journal of
Applied
Crystallography
ISSN 0021-8898

Received 14 February 2008
Accepted 17 September 2008

X-ray powder diffraction quantitative analysis of an amorphous SiO_2–poly(methyl methacrylate) nanocomposite

P. Riello,[a,c]* M. Munarin,[a] S. Silvestrini,[a] E. Moretti[b,c] and L. Storaro[b,c]

[a]Department of Physical Chemistry, Ca' Foscari University of Venice, Via Torino 155b, 30170 Venice, Italy, [b]Department of Chemistry, Ca' Foscari University of Venice, Via Torino 155b, 30170 Venice, Italy, and [c]INSTM UdR Venezia, Via Torino 155b, 30170 Venice, Italy. Correspondence e-mail: riellop@unive.it

Quantification of individual phases within a multiphase amorphous material has been achieved using a newly developed technique based on X-ray powder diffraction. The quantification method was developed during a study of an amorphous silica–poly(methyl methacrylate) (SiO_2–PMMA) hybrid nanocomposite. The efficiency of the method as a quantifying tool for individual phases was demonstrated for samples of SiO_2–PMMA prepared either by polymerization of methyl methacrylate in the presence of amorphous SiO_2 or by mechanically mixing known quantities of the individual and pre-prepared SiO_2 and PMMA materials. The weight percentages of amorphous SiO_2 in the nanocomposites as determined by application of the new technique were analogously found to be 29%, a result that was supported by thermogravimetric analysis and helium picnometry measurements.

© 2008 International Union of Crystallography
Printed in Singapore – all rights reserved

1. Introduction

Nanocomposite materials encompass a wide variety of crystalline, semicrystalline and amorphous materials constituted by dissimilar phases that are mixed on the nanometre scale. The properties exhibited by such mixed materials depend not only on the characteristics of the individual parent phases, but also on their resulting morphologies when combined and their interfacial characteristics.

As materials scientists rapidly expand the field to generate new composite materials that may potentially reveal novel properties, a significant emphasis is placed on controlling the morphologies of these materials, particularly of nanoscale structures, *via* innovative synthetic approaches. Such control, however, particularly at the nanoscale level, relies on the use of practical and accurate characterization techniques.

X-ray powder diffraction (XRPD) is routinely employed as a characterization tool by materials scientists for the study of crystalline and semicrystalline materials. Notwithstanding their indispensability as a quantitative technique in analyzing crystalline and semicrystalline materials, diffraction-based methods have thus far shown limited applicability in the analysis of amorphous composite and nanocomposite materials.

In this article we present a novel XRPD-based technique and demonstrate its use for the quantitative analysis of a hybrid nanocomposite comprising amorphous sub-micrometric silica (SiO_2) spheres that are embedded within amorphous poly(methyl methacrylate) (PMMA). Several of the techniques employed in this study were previously proposed by one of the authors and applied in the quantitative analysis of semicrystalline materials, eliminating the use of an internal standard and employing a modified Rietveld analysis (Riello, Canton & Fagherazzi, 1998). The analytical approach takes advantage of a well known property of the kinematical diffraction theory, which states that the integrated diffracted intensity of an ensemble of N atoms is an invariant and is independent of the atomic spatial order (Riello, Fagherazzi & Canton, 1998).

2. Theory

By considering a sample made of two different phases with electronic densities $\rho_1(x)$ and $\rho_2(x)$, the electronic density of the whole composite can be represented by the function

$$\rho(\mathbf{x}) = \sigma_1(\mathbf{x})\rho_1(\mathbf{x}) + \sigma_2(\mathbf{x})\rho_2(\mathbf{x}), \tag{1}$$

where the value of the function $\sigma_i(\mathbf{x})$ equals unity inside the space volume occupied by the ith phase and zero outside. The diffracted intensity $I^{\rm comp}(\mathbf{s})$ of the composite material, as a function of the scattering vector in the reciprocal space, $\mathbf{s}$, can be correlated to the Fourier transform (FT) of its electronic density:

$$\begin{aligned} I^{\rm comp}(\mathbf{s}) &= \left|{\rm FT}\left[\sigma_1(\mathbf{x})\rho_1(\mathbf{x}) + \sigma_2(\mathbf{x})\rho_2(\mathbf{x})\right]\right|^2 \\ &= \left|{\rm FT}\left[\sigma_1(\mathbf{x})\rho_1(\mathbf{x})\right]\right|^2 + \left|{\rm FT}\left[\sigma_2(\mathbf{x})\rho_2(\mathbf{x})\right]\right|^2 \\ &\quad + 2{\rm Re}\left\{{\rm FT}\left[\sigma_1(\mathbf{x})\rho_1(\mathbf{x})\right]\overline{{\rm FT}\left[\sigma_2(\mathbf{x})\rho_2(\mathbf{x})\right]}\right\} \\ &\equiv I_1(\mathbf{s}) + I_2(\mathbf{s}) + {\rm INT}(\mathbf{s}). \end{aligned} \tag{2}$$

The first two terms, $I_1(\mathbf{s})$ and $I_2(\mathbf{s})$, are the intensities of the constituting phases, while the last term, $\mathrm{INT}(\mathbf{s})$, is a cross interference term. $I_1(\mathbf{s})$ and $I_2(\mathbf{s})$ are analyzed first. Even by considering a sample composed of very small domains with a volume L^3 (*e.g.* $L \simeq 100$ nm), the diffracted intensity of each phase can be well approximated as the intensity of a macroscopic volume of the phase itself. The diffracted intensity is therefore given by the convolution ($\otimes$) of the very sharp function $|\tilde{\sigma}(\mathbf{s})|^2$ with the diffraction pattern of a virtually infinite object $I^{\infty}(\mathbf{s})$ that exhibits the same electronic density $\rho(\mathbf{x})$ (Guinier, 1963):

$$\left|\mathrm{FT}[\sigma(\mathbf{x})\rho(\mathbf{x})]\right|^2 = \mathrm{FT}[p(\mathbf{x})] \otimes |\tilde{\sigma}(\mathbf{s})|^2 \cong \mathrm{FT}[p(\mathbf{x})] \propto I^{\infty}(\mathbf{s}), \tag{3}$$

where $\tilde{\sigma}(\mathbf{s}) = \mathrm{FT}[\sigma(\mathbf{x})]$ and $p(\mathbf{x})$ is the average value of the integral $\int \rho(\mathbf{x}+\mathbf{u})\,\rho(\mathbf{u})\,\mathrm{d}\mathbf{u}$. The width of the function $|\tilde{\sigma}(\mathbf{s})|^2$ in the reciprocal space is $\Delta s \simeq 1/L$. When dealing with amorphous phases, this approximation can be applied to domains with $L < 100$ nm, since $|\tilde{\sigma}(\mathbf{s})|^2$ is convoluted with a function presenting no sharp maxima and which varies only very slowly with $\mathbf{s}$.

The diffraction intensity of an isotropic material such as the one studied is henceforth considered. Equation (2) becomes

$$I^{\mathrm{comp}}(s) = I_1(s) + I_2(s) + \mathrm{INT}(s), \tag{4}$$

with $s = |\mathbf{s}| = 2\sin(\theta)/\lambda$, 2θ being the scattering angle and λ the X-ray wavelength. In this case the diffracted intensity can be readily collected by powder diffraction analysis. If the intensities $I_1^{\infty}(s)$ and $I_2^{\infty}(s)$ can be measured for each of the individual phases, in this study SiO_2 and PMMA, that constitute the composite [and can be corrected for the absorption, polarization and air scattering phenomena in agreement with Ottani *et al.* (1993)], then $I_1(s)$ and $I_2(s)$ in equation (4) are consequently known: $I_1(s) = aI_1^{\infty}(s)$ and $I_2(s) = bI_2^{\infty}(s)$, a and b being unknown scale factors. Generally, the scattering intensity of the nanocomposite cannot be obtained as a mere linear combination of $I_1^{\infty}(s)$ and $I_2^{\infty}(s)$ owing to the interference term $\mathrm{INT}(s)$. This last term is dependent on the relative spatial distribution of the parent phases, and its functional dependence on s needs to be evaluated from the relative model. Notwithstanding this limitation, it is possible to obtain a precise evaluation of the weight fractions of the parent phases.

Previous studies have reported that, for a sample containing $N = \mathcal{N}n$ atoms, the integrated intensity over the whole reciprocal space is independent of the atomic spatial order (Riello, Fagherazzi & Canton, 1998). Assuming that the diffracted intensity $I(s)$ has been corrected for absorption, polarization and air scattering (Ottani *et al.*, 1993),

$$\begin{aligned}\int_0^{\infty} I(s)\,s^2\,\mathrm{d}s &= C\sum_1^N \int_0^{\infty}\left[|f_i^{\mathrm{o}}(s)|^2 + I_i^{\mathrm{inc}}(s)\right]s^2\,\mathrm{d}s \\ &= C\mathcal{N}\sum_1^n \int_0^{\infty}\left[|f_i^{\mathrm{o}}(s)|^2 + I_i^{\mathrm{inc}}(s)\right]s^2\,\mathrm{d}s,\end{aligned} \tag{5}$$

where the N atoms are grouped in $\mathcal{N}$ composition units, for example the molecular unit, each one composed of n atoms. C is an unknown proportionality constant, $f_i^{\mathrm{o}}(s)$ is the tabulated atomic scattering factor and $I_i^{\mathrm{inc}}(s)$ is the incoherent scattering of the ith atom (Smith *et al.*, 1975). The incoherent scattering intensity $I_i^{\mathrm{inc}}(s)$ is further corrected for the monochromator bandpass function (Riello *et al.*, 1997), since the instrument employed in the study was equipped with a monochromator for the diffracted beam. Evaluating the integral (5) for the nanocomposite results in

$$\begin{aligned}\int_0^{\infty} I^{\mathrm{comp}}(s)\,s^2\,\mathrm{d}s &= \int_0^{\infty} I_1(s)\,s^2\,\mathrm{d}s + \int_0^{\infty} I_2(s)\,s^2\,\mathrm{d}s + \int_0^{\infty}\mathrm{INT}(s)\,s^2\,\mathrm{d}s \\ &= C\mathcal{N}_1\sum_1^{n_1}\int_0^{\infty}\left[|f_i^{\mathrm{o}}(s)|^2 + I_i^{\mathrm{inc}}(s)\right]s^2\,\mathrm{d}s \\ &\quad + C\mathcal{N}_2\sum_1^{n_2}\int_0^{\infty}\left[|f_i^{\mathrm{o}}(s)|^2 + I_i^{\mathrm{inc}}(s)\right]s^2\,\mathrm{d}s.\end{aligned} \tag{6}$$

$\mathcal{N}_1$ and $\mathcal{N}_2$ correspond to the number of molecules of PMMA and of SiO_2 in the sample, respectively, n_1 and n_2 being the numbers of atoms in such molecules. Therefore, by taking into account that $I_1(s)$ and $I_2(s)$ are the given intensities of the two individual phases,

$$\int_0^{\infty} I_l(s)\,s^2\,\mathrm{d}s = C\mathcal{N}_l\sum_1^{n_l}\int_0^{\infty}\left[|f_i^{\mathrm{o}}(s)|^2 + I_i^{\mathrm{inc}}(s)\right]s^2\,\mathrm{d}s, \tag{6a}$$

where the subscript l denotes the lth phase. Comparison of equations (6) and (6a) gives

$$\int_0^{\infty}\mathrm{INT}(s)\,s^2\,\mathrm{d}s = 0. \tag{7}$$

By determining the contribution towards the overall scattering $I^{\mathrm{comp}}(s)$ that arises from each component $I_1(s)$ and $I_2(s)$, the number of the composition units $\mathcal{N}_l$ and the weight fraction W_l of the individual parent phases can be subsequently calculated using equations (8), thus permitting the desired quantitative analysis:

$$C\mathcal{N}_l = \frac{\int_0^{\infty} I_l(s)\,s^2\,\mathrm{d}s}{\sum_1^{n_l}\int_0^{\infty}\left[|f_i^{\mathrm{o}}(s)|^2 + I_i^{\mathrm{inc}}(s)\right]s^2\,\mathrm{d}s}, \tag{8a}$$

$$W_l = \frac{C\mathcal{N}_l\sum_{i=1}^{n_l} w_l^i}{\sum_{l=1}^{N_{\mathrm{phase}}} C\mathcal{N}_l\sum_i^{n_l} w_l^i}, \tag{8b}$$

where w_l^i is the atomic weight of the ith atom of the lth phase and N_{phase} is the number of phases constituting the sample (two in this study). It is worth observing that the unknown proportionality constant C in equations (8a) and (8b) is the same for each of the phases in the sample.[1] Additionally, it should be noted that, in order to apply this method, precise knowledge of the chemical composition, *i.e.* the constituting phases present, is essential for calculation of W_l. Furthermore, since the integrals in these equations are extended towards the

[1] Factor C may be phase-dependent, if micro-absorption is taken into account (Taylor & Matulis, 1991).

whole reciprocal space, despite the diffraction data being accessible solely in the finite range $s_{\min} < s < s_{\max}$, $\mathcal{CN}_l$ is evaluated as the asymptotic value of the function $\mathcal{CN}_l(s_p)$:

$$\mathcal{CN}_l = \lim_{s_p\to\infty} \mathcal{CN}_l(s_p) = \lim_{s_p\to\infty} \frac{\int_{s_{\min}}^{s_p} I_l(s)\, s^2\, ds}{\sum_1^{n_l} \int_{s_{\min}}^{s_p} \left[f_i^o(s) + I_i^{\rm inc}(s)\right] s^2\, ds}, \quad (8c)$$

which is approximated with the average value of the function $\mathcal{CN}(s_p)$ in the range $s_p > 1$ Å^{-1}. Finally, as a consequence of the weighting factor s^2, the value of $s_{\min}$ is not a crucial factor if the starting angle is not too large.

In order to apply the procedure described thus far, the terms $I_1(s)$, $I_2(s)$ and INT(s) in the expression for $I^{\rm comp}(s)$ [equation (4)] need to be separated. This can be achieved by performing a constrained least-squares fit of the measured intensity of the composite $I^{\rm comp}(s)$ as a linear combination of the measured intensities of the constituting phases $I_1(s)$ and $I_2(s)$ (in this study, SiO_2 and PMMA, respectively). The process involves finding the minimum of the $\chi^2(a, b, \alpha)$ function with respect to the parameters a, b and the Lagrange multiplier α:

$$\chi^2(a, b, \alpha) = \sum_i \left[I^{\rm comp}(s) - aI_1^\infty(s) - bI_2^\infty(s)\right]^2 + \alpha \sum_i \left[I^{\rm comp}(s_i) - aI_1^\infty(s_i) - bI_2^\infty(s_i)\right] s_i^2\, ds_i. \quad (9)$$

In this article, $I^{\rm comp}(s)$, $I_1^\infty(s)$ and $I_2^\infty(s)$ refer to the measured intensities of the composite material, SiO_2 and PMMA, respectively. Owing to the linearity of the problem it is very easy to find the minimum of χ^2.

The introduction of the Lagrange multiplier α forces the fitting procedure to look for a solution where

$$\sum_i \left[I(s_i) - aI_1^\infty(s_i) - bI_2^\infty(s_i)\right] s_i^2\, ds_i = \int \left[I(s) - aI_1^\infty(s) - bI_2^\infty(s)\right] s^2\, ds \equiv \int {\rm INT}(s)\, s^2\, ds = 0. \quad (10)$$

At this point, the use of the least-squares fitting process merits a brief explanation. It must be noted that the 'best fit' of the data in a conventional sense is not the aim of the proposed procedure. The objective of this study is to obtain a coherent separation of the intensities arising from the parent phases rather than a microstructural model of the composite, thus allowing their quantitative determination. Statistical indexes such as the goodness of fit (GOF) may indicate a wide range of values for materials of the same composition yet with differing microstructure. Consequently, the GOF index loses its intended meaning here and thus cannot be used to evaluate the reliability of the analysis. The GOF value depends on the microstructural details determining the functional shape of the interference term INT(s), which is the main contribution to the residual of the fit.

To summarize, the proposed method simply allows us to measure the contribution given by the individual $I_1(s)$ and $I_2(s)$ phase components against the overall integrated scattering of the composite, ensuring the coherence of the separation. This method cannot give information concerning the microstructure of the nanocomposite, but provides rather a precise determination of its phase composition. The feasibility of achieving the latter is presented here as a quantitative evaluation of an amorphous SiO_2–PMMA hybrid nanocomposite.

3. Experimental

3.1. Synthesis of SiO_2 Stöber nanoparticles

Silica particles were prepared using the precursor tetraethoxysilane (TEOS) according to the modified Stöber synthesis described by Buining & Philipse (1996). The respective molar ratios of reagents were 1TEOS:7.5H_2O:1.5NH_4OH:34EtOH. The obtained silica spheres were dried overnight at 400 K.

3.2. Synthesis of PMMA nanoparticles

Spherical PMMA particles were synthesized *via* a microemulsion method according to the procedure of Zou *et al.* (1992).

3.3. Synthesis of SiO_2–PMMA nanocomposite

A suspension of SiO_2 (3.3 mmol) in methyl methacrylate (1 mol) was magnetically stirred and sonicated for 5 min. The surfactant Tergitol 15-S-12 (5 mmol) was then added and the suspension was sonicated for an additional 2 min. Deionized water (31.7 mol) was added to the suspension and the temperature was stabilized at 348 K under an N_2 atmosphere. The radical initiator 2,2′-azobis(2-methylpropionamidine) dihydrochloride (2.4 mmol) was quickly added to the suspension, and stirring was continued at 348 K for 40 min. The polymerization was then quenched by exposure to air. The resulting product, herein referred to as COMP, was recovered by centrifugation and dried overnight.

A second sample, named MIX, prepared with the same weight fraction of silica (as that of COMP) was prepared by means of mechanical mixing *via* mild milling of SiO_2 and PMMA spheres.

3.4. Characterization techniques

XRPD patterns were recorded at room temperature with a step size of 0.05° in the 5–140° range. The diffraction data were collected (10 s step^{-1}) using a Philips X'Pert system (PW3020 vertical goniometer and PW3710 MPD control unit) equipped with a focusing graphite monochromator on the diffracted beam and with a proportional counter (PW1711/90) with electronic pulse height discrimination. A 0.5° divergence slit was used, together with a receiving slit of 0.2 mm, an anti-scatter slit of 0.5° and Ni-filtered Cu $K\alpha$ radiation (30 mA, 40 kV).

The composite and the parent phases (PMMA and SiO_2) were further characterized by thermogravimetric analysis (TGA; Netzcsh STA 409) with a heating rate of 10 K min^{-1},

while their true densities were evaluated by helium pycnometry (multivolume pycnometer 1305 by Micrometric).

Transmission electron microscopy (TEM) images were taken with a Jeol JEM-3010, operating at 300 kV, equipped with a GATAN (Warrendale, PA, USA) MultiScan CCD camera model 794. A Gatan 613-DH specimen holder was used to cool the specimen to liquid nitrogen temperature, in order to keep it stable under the electron beam.

Scanning electron microscopy (SEM) images were recorded with a Jeol JSM-5600LV, operated at 20 kV and using secondary electrons to form the image. The sample was coated with a thin layer of gold.

4. Results and discussion

Figs. 1(*a*) and 1(*b*), respectively, show the near spherical PMMA particles obtained by the micro-emulsion method and the silica spheres obtained by the modified Stöber method. The microstructure of the nanocomposite material COMP can be observed in the TEM image presented in Fig. 2.

The TGA profiles of the parent materials and COMP are displayed in Fig. 3. A maximum 15% weight loss is observed at 420 K for SiO_2, which is attributed to the elimination of the residual organic solvent and physisorbed water. Evidently, the extended thermal treatment of SiO_2 at 400 K following its synthesis leads to the weight stabilization that is observed above 420 K. In contrast, degradation of PMMA commences at 520 K and is complete at 690 K; a slight weight loss prior to 520 K may be attributed to the presence of residual solvent. On the other hand, the TGA of the hybrid COMP shows slower degradation kinetics in comparison with that of PMMA. After a slight initial weight loss from the elimination of residual solvent, thermal degradation of COMP occurs in the 470–700 K range (excluding a small stabilization which can be noted in the 700–1100 K range). This difference in weight loss between PMMA and COMP allows for a simple quantitative measurement to be made, from which a value of 29 wt%

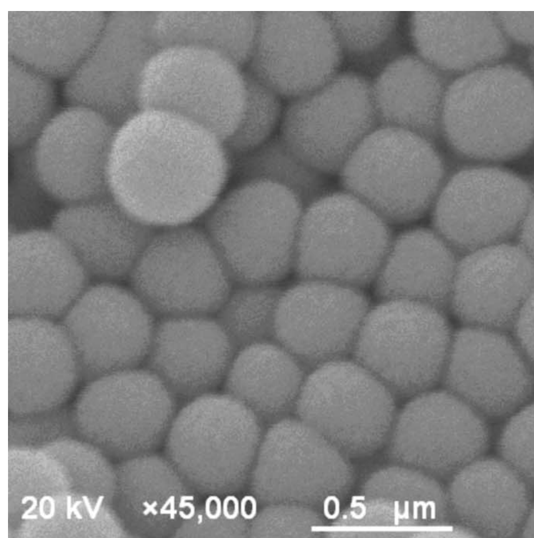

(*a*)

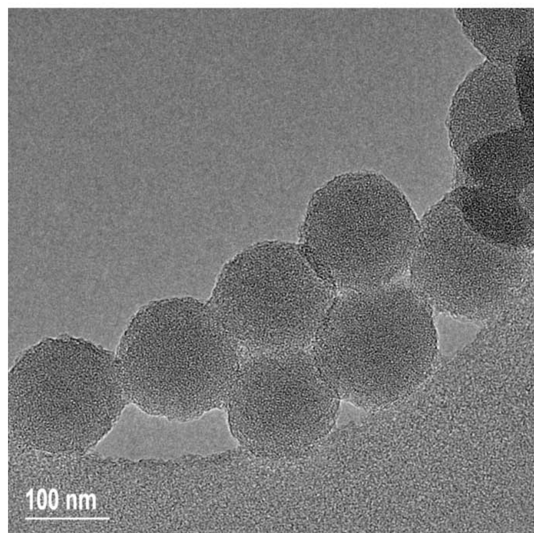

(*b*)

Figure 1
(*a*) SEM micrograph of the pure PMMA obtained by the micro-emulsion method. (*b*) TEM micrograph of silica particles obtained by the Stöber method.

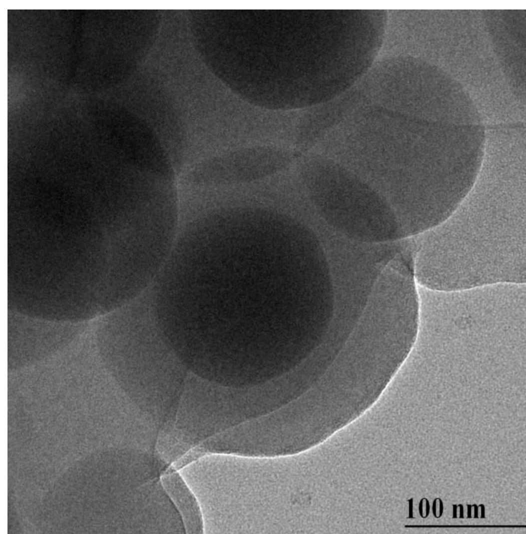

Figure 2
TEM micrograph of the nanocomposite sample COMP.

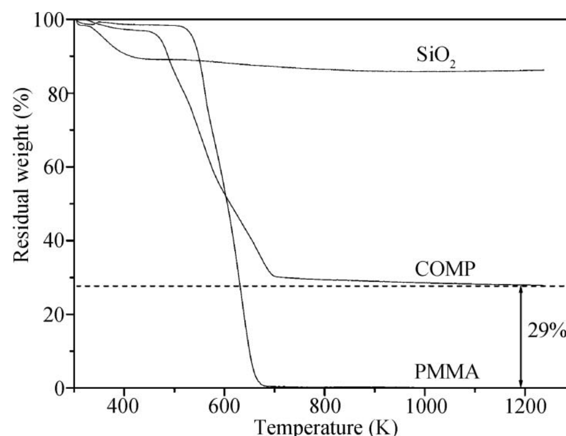

Figure 3
TGA curves for SiO_2, COMP and PMMA.

Table 1
Mass densities of the samples.

Sample	True density (g cm^{-3})
SiO_2	1.81 (1)
PMMA	1.20 (2)
COMP	1.33 (1)

of SiO_2 in the composite is derived. Corresponding results are obtained by mass density measurements. The measured mass densities of the three different samples are reported in Table 1. It is clearly shown that the density of COMP corresponds to the expected density of a sample containing 71 wt% PMMA and 29 wt% SiO_2.

MIX was prepared by mechanically mixing SiO_2 and PMMA nanospheres to give an SiO_2:PMMA weight ratio [29.0 (2) wt% SiO_2] in agreement with that of COMP. In Fig. 4, corrected diffraction patterns for all samples are shown in arbitrary units. Figs. 5(*a*) and 5(*b*) compare the patterns of COMP and MIX with the linear combinations of the patterns obtained for PMMA and SiO_2 by the constrained least-squares fit.

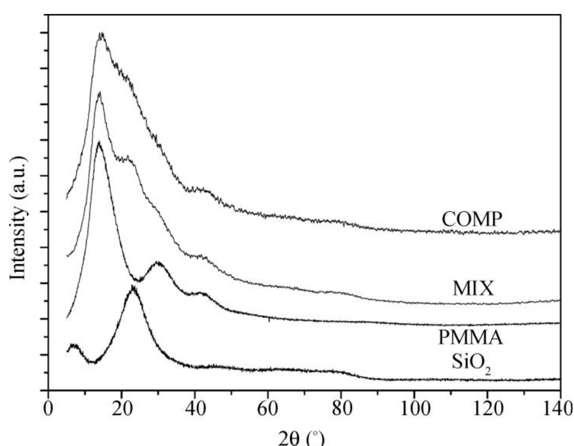

Figure 4
XRPD patterns of the samples COMP and MIX and their individual components. The patterns are vertically shifted to improve the visual clarity of the figure.

The components $I_1(s)$ and $I_2(s)$ (named a*SiO_2 and b*PMMA, respectively, in Fig. 5) are used to evaluate the weight (in arbitrary units) of SiO_2 and PMMA within the samples COMP and MIX as asymptotic values of the functions

$$C\mathcal{N}_l(s_p)\sum_{i=1}^{n_l} w_l^i = \frac{\int_{s_i}^{s_p} I_l(s)\, s^2\, ds}{\sum_1^{n_l}\int_0^{\infty}\left[f_i^o(s) + I_i^{inc}(s)\right] s^2\, ds}\sum_{i=1}^{n_l} w_l^i, \qquad (11)$$

which are illustrated in Fig. 6. The obtained weight fractions of SiO_2 in COMP and MIX are 0.290 and 0.305, respectively. These values agree closely with the previously measured value of 0.29 for COMP obtained by TGA and helium pycnometry (Fig. 3 and Table 1) and the theoretical amount measured by directly weighting the parent components in MIX [0.290 (2)]. The small discrepancy between the values obtained by XRPD and the expected value for the mixed sample MIX can be ascribed to a lower homogeneity of this sample in comparison with the composite COMP.

In spite of the identical composition, the patterns of the two samples are different (see Fig. 5). The differences are related to the local distribution of the two parent phases, and the XRPD pattern of the sample obtained by mixing (MIX) is better described by the linear combination of the SiO_2 and PMMA patterns. Although the two samples have a different cross interference term INT(*s*), the analysis yields accurate quantitative results.

5. Conclusions

In the present study, a new XRPD-based procedure for the quantitative evaluation of individual amorphous phases within a completely amorphous material was developed. The effectiveness of the proposed methodology was demonstrated for

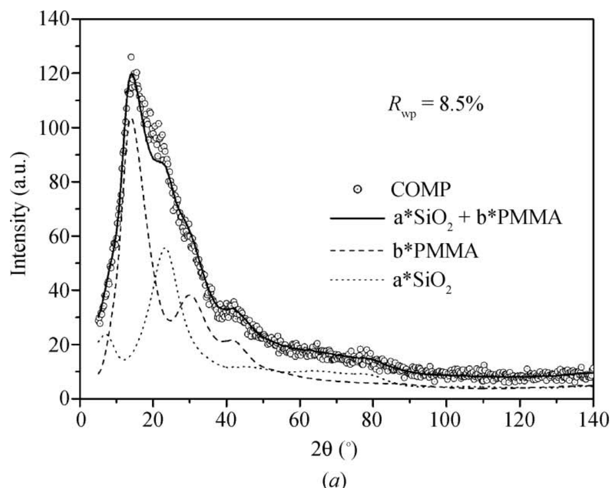

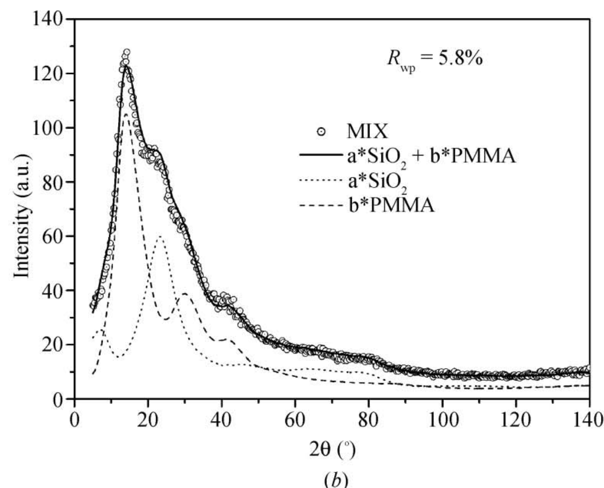

Figure 5
Results of the fitting procedure; the XRPD patterns of the samples COMP (*a*) and MIX (*b*) are compared with the linear combination of the patterns of SiO_2 and PMMA.

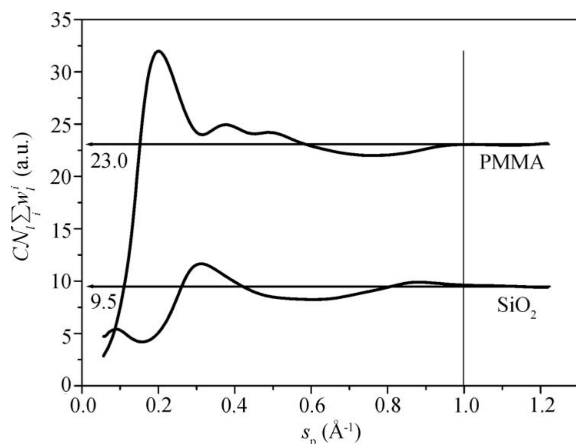

Figure 6
Evaluation of the weights (in arbitrary units) of the two fractions constituting the nanocomposite COMP; the functions $C\mathcal{N}_l(s_p)\sum_{i=1}^{n_l} w_l^i$ are plotted and their asymptotic values are estimated as the average values of the functions in the range $s_p > 1$ Å^{-1}.

an amorphous nanocomposite which comprised SiO_2 and PMMA phases. On the basis of an earlier concept (Riello, Canton & Fagherazzi, 1998), which was successfully applied in the quantitative analysis of semicrystalline samples in the absence of an internal standard, the method proved to be similarly applicable and highly useful in the study of fully amorphous composites. The method allowed the quantification of individual phases within an amorphous SiO_2–PMMA nanocomposite, and the results were corroborated by TGA and picnometry measurements. The new procedure can be applied when the chemical composition and the XRPD patterns of all the present phases in the composite are obtainable, and it may be easily extended to an arbitrary number of components.

References

Buining, P. A. & Philipse, A. P. (1996). *J. Colloid Interface Sci.* pp. 318–321.
Guinier, A. (1963). *X-ray Diffraction in Crystals, Imperfect Crystals, and Amorphous Bodies*, p. 41. San Francisco: W. H. Freeman and Company, and Dover.
Ottani, S., Riello, P. & Polizzi, S. (1993). *Powder Diffr.* **8**, 149–154.
Riello, P., Canton, P. & Fagherazzi, G. (1997). *Powder Diffr.* **12**, 160–166.
Riello, P., Canton, P. & Fagherazzi, G. (1998). *J. Appl. Cryst.* **31**, 78–82.
Riello, P., Fagherazzi, G. & Canton, P. (1998). *Acta Cryst.* A**54**, 219–224.
Smith, V. H., Thakkar, A. J. & Chapman, D. C. (1975). *Acta Cryst.* A**31**, 391–392.
Taylor, J. C. & Matulis, C. E. (1991). *J. Appl. Cryst.* **24**, 14–17.
Zou, D., Ma, S., Guan, R., Park, M., Sun, L., Aklonis, J. J. & Salovey, R. (1992). *J. Polym. Sci. Part A Polym. Chem.* **30**, 137–144.